ARTICLE

OBC
www.rsc.org/obc

Control of rotor motion in a light-driven molecular motor: towards a molecular gearbox

Matthijs K. J. ter Wiel, Richard A. van Delden, Auke Meetsma and Ben L. Feringa*

Department of Organic and Molecular Inorganic Chemistry, Stratingh Institute, University of Groningen, Nijenborgh 4, 9747, AG Groningen, The Netherlands. E-mail: b.l.feringa@rug.nl; Fax: +31 50 363 4296; Tel: +31 50 363 4278

Received 26th July 2005, Accepted 20th September 2005
First published as an Advance Article on the web 17th October 2005

Controlled intramolecular movement and coupling of motor and rotor functions is exerted by this new molecular device. The rate of rotation of the rotor part of the molecule can be adjusted by alteration of the conformation of the motor part of the molecule. For all states of the motor part, different rates of rotation were measured for the rotor part. Conversion between the four propeller orientations was achieved by irradiation and heating.

Introduction

The construction of artificial molecular machines is one of the major contemporary challenges in nanoscience.[1] The functioning of these machines will critically depend on the ability to power and control rotary movement like in the macroscopic motors used in daily life and the rotary motors present in biological machines, most elegantly seen in ATP synthase.[2] The synthesis of molecular motors and the demonstration of unidirectional rotary motion driven by light or chemical conversions has laid the foundation for future nanomotors.[3] The studies on geared propeller structures[4] and a variety of elegant molecular rotors[5] paved the way to systems in which several rotary units are coupled. In this manuscript we describe a molecular device in which controlled movement in a molecular motor is used to control the rotary motion of a second rotor function in the system.

Results and discussion

Our design is based on the second-generation light-driven unidirectional molecular motors **1** (Fig. 1).[6]

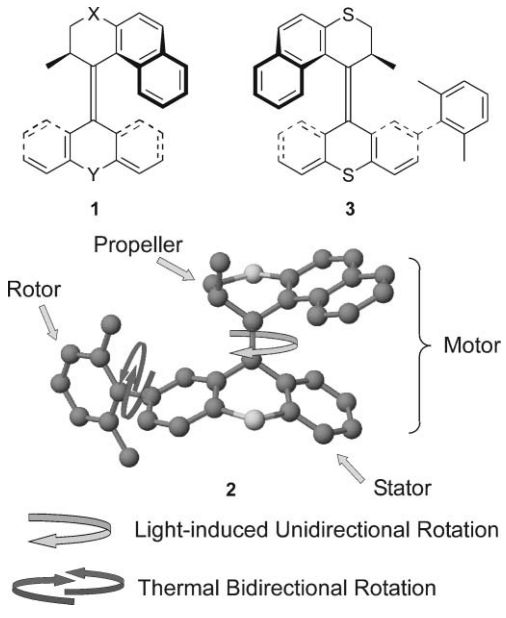

Fig. 1 The molecular motor–rotor system based on a sterically overcrowded alkene.

To the lower (stator) part of the molecular motor in **2**, a rotor is attached and the controlled rotary movement of the upper propeller part is envisioned to govern the rotation of the rotor unit. As a target, compound **3** was designed. We designate this system as a molecular gearbox since the position of the upper propeller part of the motor during the 360° rotation is expected to allow control over the speed of rotation of the *o*-xylyl cogwheel (rotor) present in the lower half.

The key-step in the synthesis of **3** was performed using the Barton–Kellogg coupling that has been used extensively for the preparation of overcrowded alkenes (Scheme 1).[6,7] Starting from hydrazone **4**[6] and thioketone **5**,[5c,6] episulfide **6** was obtained in excellent yield and subsequent treatment with triphenylphosphine provided alkene **3** as a mixture of *cis–trans* isomers in a ratio of 3.5 : 1.[8]

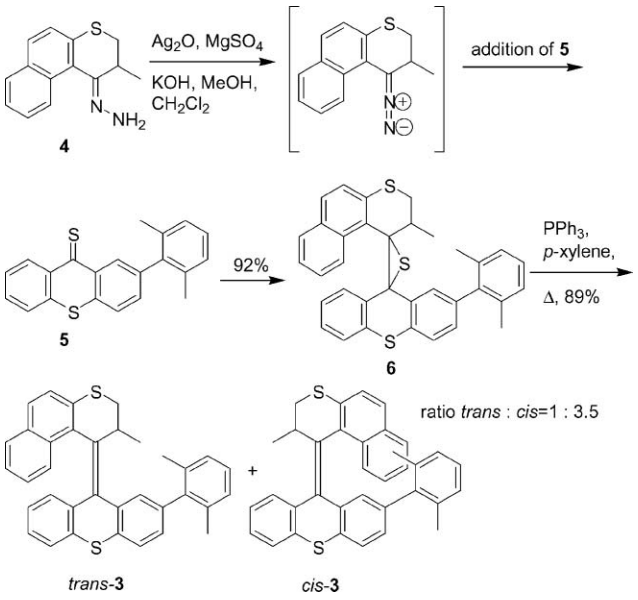

Scheme 1 Synthesis of the molecular gearbox **3**.

By slow evaporation of an *n*-hexane solution containing **3** as a *cis–trans* mixture, small colorless crystals of (2′*S**)-(*P**)-*trans*-**3**[9] were obtained that proved to be suitable for X-ray analysis (Fig. 2). From the structure the helical shape of the molecule is apparent, but more importantly, it can be seen clearly that the methyl substituent preferentially adopts a (pseudo-)axial orientation.

DOI:10.1039/b510641a

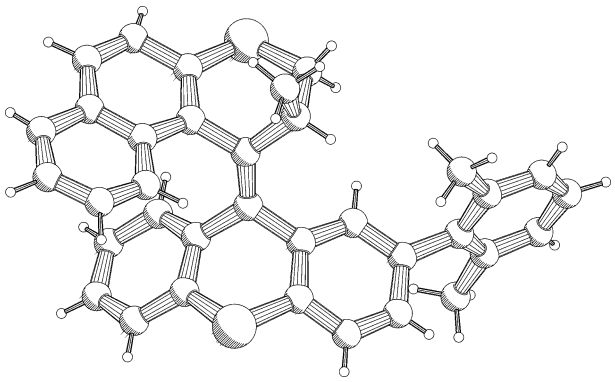

Fig. 2 Pluto drawing of (2′*S**)-(*P**)-*trans*-**3**.[10] The picture does not represent the absolute configuration of the molecule.

In the ^{1}H NMR spectra of (2′*S**)-(*P**)-*cis*-**3**[9] and (2′*S**)-(*P**)-*trans*-**3** in $CDCl_3$, the absorptions originating from the two methyl substituents of the *o*-xylyl moiety appear as separate singlets for both isomers. Due to the steric crowding in the molecule, on the NMR timescale only a slow exchange between the two is possible at ambient temperature. For the *o*-xylyl methyl protons of (2′*S**)-(*P**)-*trans*-**3**, two singlets are observed at δ 1.97 and 2.22 ppm and for (2′*S**)-(*P**)-*cis*-**3** these methyl absorptions are found at higher field and appear as two singlets at δ 0.77 and 1.69 ppm. Fortunately, there is no overlap with the six alkyl protons of the upper half. The doublet of the methyl substituent attached to the stereogenic center was found at δ 0.81 ppm for (2′*S**)-(*P**)-*trans*-**3** and at δ 0.67 ppm for (2′*S**)-(*P**)-*cis*-**3**. The position of these absorptions is important to determine whether the methyl substituent is in a stable axial or an unstable equatorial orientation.[6]

As was known from earlier studies performed with a molecular rotor,[5c] coalescence measurements using ^{1}H NMR are not suitable to determine the rotation rate of the *o*-xylyl moiety due to the high barrier of activation. Since similar barriers were expected for **3**, 2D EXSY spectroscopy was performed to determine the rate of rotation of the *o*-xylyl moiety. The *o*-xylyl moiety is well suited for an EXSY-experiment since it behaves as a two-site exchange system.[11,12] The advantages of this two-state system are that the populations are equal and that the spin–lattice relaxation time is, within error margins, the same for both methyl substituents. It is important to record spectra with different mixing times (t_m) at each temperature in order to measure the exchange process in the initial rate regime.

EXSY spectra were recorded at 25, 35, 45 and 55 °C with a mixture containing both stable (2′*S**)-(*P**)-*trans*-**3** and stable (2′*S**)-(*P**)-*cis*-**3** to ensure identical conditions for the different isomers. At each temperature, different mixing times (typical values of t_m were 0.05, 0.1, 0.2, 0.3, 0.5, 0.7, 1.0 and 1.5 s) were used and care was taken to use only data obtained in the initial rate regime.[13] For (2′*S**)-(*P**)-*trans*-**3** and (2′*S**)-(*P**)-*cis*-**3**, the results of these measurements are shown in Figs. 3 and 4. From the slope of the plot of t_m *versus* ($a_{AB}/(a_{AA} + a_{AB})$) the rate constant *k* at each temperature was determined (Figs. 3 and 4).

In order to be able to determine the rates of rotation of the *o*-xylyl rotor moiety for the unstable isomers of **3**, (2′*S**)-(*M**)-*trans*-**3** and (2′*S**)-(*M**)-*cis*-**3**, a mixture of the stable isomers of **3** was irradiated for 1 h ($\lambda \geq 280$ nm, $T = 20$ °C) in $CDCl_3$.[14] Moreover, both unstable forms of **3** are sufficiently stable to allow measurements at temperatures up to 55 °C.

That indeed the unstable forms with equatorial methyl substituents were generated was concluded from the shifts in the ^{1}H NMR spectrum of the absorptions of the methyl substituents in the upper half of the molecules, which in the unstable forms of the second-generation motors are situated at lower field compared to the stable forms.[6] For (2′*S**)-(*P**)-*cis*-**3** compared to (2′*S**)-(*M**)-*cis*-**3**, a shift from δ 0.66–0.68 ppm to δ 1.09–1.12 ppm was observed, and for (2′*S**)-(*P**)-*trans*-**3** compared

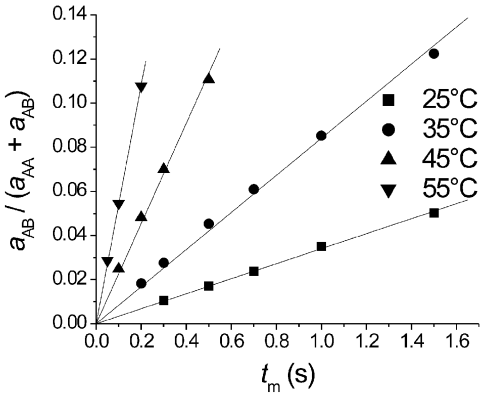

Fig. 3 Graph showing the relation between the mixing time (t_m) and the cross-(a_{AB}) and autopeaks (a_{AA}) for stable *trans*-**3**.

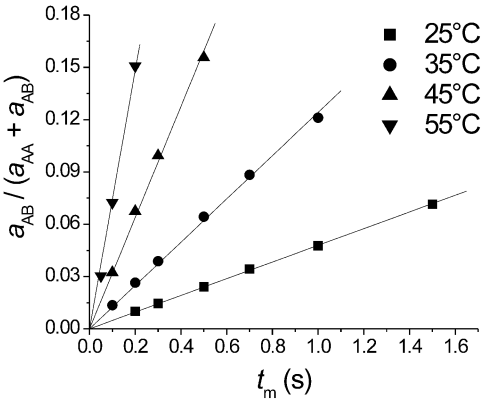

Fig. 4 Graph showing the relation between the mixing time (t_m) and the cross-(a_{AB}) and autopeaks (a_{AA}) for stable *cis*-**3**.

to (2′*S**)-(*M**)-*trans*-**3**, a shift from δ 0.80–0.82 ppm to δ 1.26–1.28 ppm was observed. The geometry around the double bond was evident from the absorptions of the methyl substituents of the *o*-xylyl part. For the stable isomers, the signals at high field are assigned to (2′*S**)-(*P**)-*cis*-**3** and at lower field to (2′*S**)-(*P**)-*trans*-**3**. For the absorption of the unstable (2′*S**)-(*M**)-*trans*-**3** and (2′*S**)-(*M**)-*cis*-**3** isomers, the same order is valid; at δ 0.55 and 1.70 ppm the absorptions of the unstable (2′*S**)-(*M**)-*cis*-**3** are found and at δ 1.92 and 2.26 ppm the absorptions of the *o*-xylyl methyl substituents for unstable (2′*S**)-(*M**)-*trans*-**3** appear. As for the stable forms of **3**, the EXSY experiments for the unstable isomers were performed at 25, 35, 45 and 55 °C. For each temperature, different mixing times were used varying typically from $t_m = 0.05$ to 1.5 s. Using the same procedures as for the stable isomers of **3**, the rate constants *k* were determined for each temperature.[15] For each of the four isomers the rate constants at each temperature are depicted in Fig. 5.

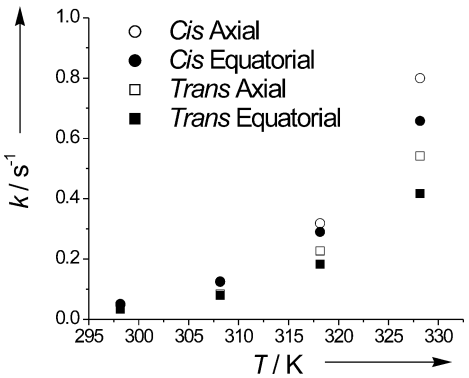

Fig. 5 The rate constants as a function of temperature of the rotation around the aryl–aryl single bond for all four isomers.

Table 1 Thermodynamic constants for all four isomers of gearbox **3**

	$\Delta^{\ddagger}G^{0}$ (kJ mol^{-1})[a]	$\Delta^{\ddagger}H^{0}$ (kJ mol^{-1})	$\Delta^{\ddagger}S^{0}$ (J K^{-1} mol^{-1})
Stable (2′*S**)-(*P**)-*cis*-**3**	81 ± 2	74 ± 1	−23 ± 4
Unstable (2′*S**)-(*M**)-*cis*-**3**	80 ± 2	66 ± 2	−47 ± 5
Stable (2′*S**)-(*P**)-*trans*-**3**	81 ± 2	73 ± 2	−28 ± 5
Unstable (2′*S**)-(*M**)-*trans*-**3**	83 ± 2	64 ± 2	−59 ± 5

[a] $T = 293.15$ K.

From Fig. 5 it becomes clear that all four isomers of **3** have a different rate of rotation around the single aryl–aryl bond between the *o*-xylyl moiety and the stator lower part of the molecule. The trend in the rate of rotation becomes especially clear at somewhat higher temperatures (45 and 55 °C) where the order is $cis_{stable} > cis_{unstable} > trans_{stable} > trans_{unstable}$ going from high to low rates. It is interesting to note, and perhaps counter intuitive, that both the stable and unstable *cis*-**3** isomers show faster rotation than the stable and unstable *trans*-**3** isomers.[16] Furthermore, it should be noted that both unstable isomers show slower rotation than the corresponding stable isomers. This is probably due to the increased steric hindrance enforced onto the *o*-xylyl moiety by the upper-part methyl substituent in the pseudo-equatorial orientation. This is supported by the thermodynamic data obtained from the Eyring plots (Table 1); the entropy of activation for the isomers with the methyl substituents in an equatorial orientation (unstable isomers) is much larger than for the isomers with the methyl substituents in an axial orientation (stable isomers). These data suggest that the change in conformation required for rotation in the unstable forms is larger than for the stable forms.

Detailed examination of the photochemical and thermal response of **3** is important, since by using these external stimuli, control over the mechanical motion can be achieved. For the investigation of the dynamic behavior of **3**, isomerically pure solutions of (2′*S**)-(*P**)-*cis*-**3** and (2′*S**)-(*P**)-*trans*-**3** in benzene-d_6 were irradiated ($\lambda \geq 280$ nm, $T = 20$ °C) (Scheme 2). The characteristic signals in the ^{1}H NMR of stable (2′*S**)-(*P**)-*trans*-**3** are a doublet at δ 0.57 ppm of the methyl moiety in the upper half of the molecule and two singlets originating from the xylyl moiety at δ 1.80 and 2.19 ppm. The same signals for stable (2′*S**)-(*P**)-*cis*-**3** are found at δ 1.04 and 1.56 ppm and the doublet of the methyl moiety of the upper half is found at δ 0.43 ppm. As was the case in chloroform, the chemical shift

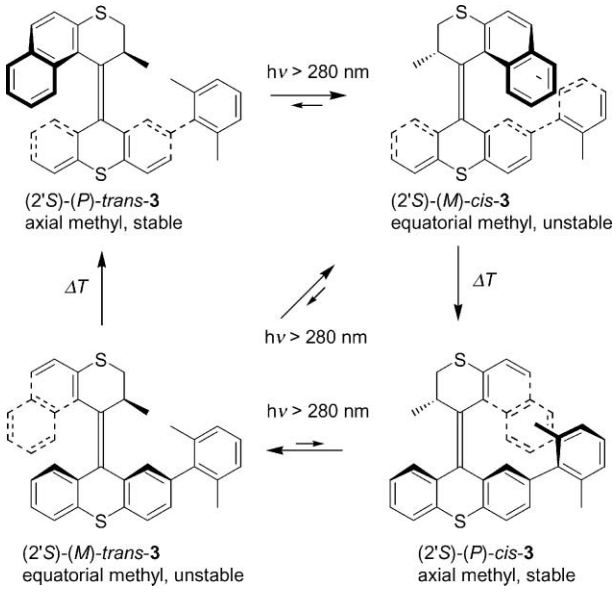

Scheme 2 The rotational scheme for molecular gearbox **3**.

difference of the two singlet signals is smaller for stable (2′*S**)-(*P**)-*trans*-**3** than for stable (2′*S**)-(*P**)-*cis*-**3**. Upon irradiation of stable (2′*S**)-(*P**)-*trans*-**3**, a shift of the absorptions of the two methyl signals from δ 1.80 and 2.19 ppm to δ 1.02 and 1.52 ppm was observed. The doublet was shifted to slightly lower field from δ 0.57 ppm to 0.80 ppm. From these data and similar observations on related second generation molecular motors,[6] it was evident that unstable (2′*S**)-(*M**)-*cis*-**3** had been formed. The shift to higher field of the two *o*-xylyl methyl singlets confirms the formation of a *cis*-isomer of **3** not identical to stable (2′*S**)-(*P**)-*cis*-**3**. Closer observation of the spectrum showed that the conversion to the unstable (2′*S**)-(*M**)-*cis*-**3** was not complete and a small amount of the stable (2′*S**)-(*P**)-*trans*-**3** was still present in the mixture. Moreover, small signals at δ 1.00 and 1.65 ppm indicate that another isomer, unstable (2′*S**)-(*M**)-*trans*-**3**, had been formed (*vide infra*). Irradiation of stable (2′*S**)-(*P**)-*cis*-**3** ($\lambda \geq 280$ nm, $T = 20$ °C) resulted initially in a shift of the methyl signals at δ 1.04 and 1.56 ppm to δ 1.65 and 2.19 ppm. The doublet signal shifted from δ 0.43 ppm to 1.00 ppm. From these two observations it was concluded that the newly formed isomer was the unstable (2′*S**)-(*M**)-*trans*-**3** isomer (Scheme 2). Longer irradiation of the sample, however, led to a slow conversion of the unstable (2′*S**)-(*M**)-*trans*-**3** to the unstable (2′*S**)-(*M**)-*cis*-**3** isomer. Eventually, upon longer irradiation the same isomeric mixture was obtained from the irradiation of stable (2′*S**)-(*P**)-*trans*-**3** or stable (2′*S**)-(*P**)-*cis*-**3**. Although in either mixture some stable (2′*S**)-(*P**)-*trans*-**3** could be observed, the amount of stable (2′*S**)-(*P**)-*cis*-**3** was too small to be detected by ^{1}H NMR. This is due to the unfavorable photoequilibrium for formation of stable (2′*S**)-(*P**)-*cis*-**3**. The ratio between the four isomers (shown in Scheme 2) was in the photostationary state (PSS): unstable (2′*S**)-(*M**)-*cis*-**3** : unstable (2′*S**)-(*M**)-*trans*-**3** : (2′*S**)-(*P**)-stable *cis*-**3** : (2′*S**)-(*P**)-stable *trans*-**3** = 90 : 6 : 0 : 4, as determined by ^{1}H NMR spectroscopy. This behavior contrasts with the original second generation molecular motor, where no direct photochemical conversion from unstable *trans* to unstable *cis* was observed. Prolonged heating of the PSS mixture leads to a conversion of the unstable isomers to the stable isomers and hence in this case to a mixture of stable (2′*S**)-(*P**)-*cis*-**3** and stable (2′*S**)-(*P**)-*trans*-**3** in a ratio of 90 : 10.[17]

The photochemical behavior of enantiomerically pure **3** was also examined by UV–Vis and CD spectroscopy in *n*-hexane. The UV–Vis and CD spectra of both stable (2′*S*)-(*P*)-*cis*-**3** and stable (2′*S*)-(*P*)-*trans*-**3** in *n*-hexane solution are depicted in Fig. 6. After the irradiation ($\lambda \geq 280$ nm, $T = 0$ °C) of stable (2′*S*)-(*P*)-*cis*-**3** or stable (2′*S*)-(*P*)-*trans*-**3**, identical UV–Vis and CD spectra were recorded. Although in the UV–Vis almost no changes were observed, the CD spectra were nearly inverted. This indicates that upon irradiation, a helix inversion occurs going from an overall (*P*)-helix before irradiation to an overall (*M*)-helix after irradiation. The fact that after irradiation of either isomer of **3** the same UV–Vis and CD spectra were obtained, indicates that the PSS has the same composition, which is in agreement with the observation by ^{1}H NMR spectroscopy (*vide supra*).

The barrier for the thermal isomerization going from the unstable (pseudo-)equatorial isomers of **3** to the stable

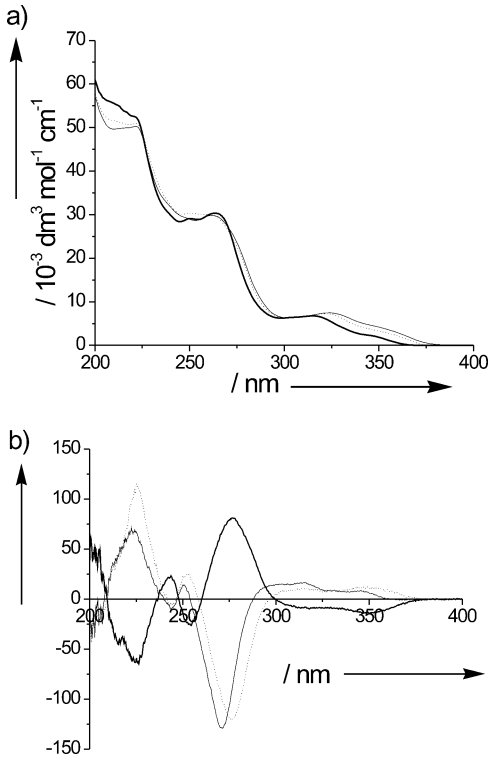

Fig. 6 UV–Vis (a) and CD spectra (b) of the stable (2′*S*)-(*P*)-*trans*-**3** (solid), stable (2′*S*)-(*P*)-*cis*-**3** (dotted) and the photostationary state mixture (thick solid).

(pseudo-)axial isomers of **3** is relatively high, but the isomerizations are quantitative and stereoselective.[18]

As the thermal isomerization steps (*i.e.* (2′*S*)-(*M*)-*cis*-**3** to (2′*S*)-(*P*)-*cis*-**3** and (2′*S*)-(*M*)-*trans*-**3** to (2′*S*)-(*P*)-*trans*-**3**) are unidirectional, the system functioning as a unidirectional rotary motor is not compromised. In the case of **3**, the 360° rotation cycle in four stages is more complicated by unexpected photochemical behavior. As was demonstrated experimentally by ^{1}H NMR spectroscopy in benzene-d_6 and confirmed by CD spectroscopy, a third photochemical isomerization occurs in which the unstable (2′*S*)-(*M*)-*trans*-**3** is converted to the unstable (2′*S*)-(*M*)-*cis*-**3**. The photoequilibrium of this process is nearly completely on the side of the unstable (2′*S*)-(*M*)-*cis*-**3**. Upon irradiation of a sample of either stable (2′*S*)-(*P*)-*cis*-**3** or stable (2′*S*)-(*P*)-*trans*-**3**, a fast photochemical equilibration occurs, resulting in a mixture of unstable (2′*S*)-(*M*)-*cis*-**3** : unstable (2′*S*)-(*M*)-*trans*-**3** : (2′*S*)-(*P*)-stable *cis*-**3** : (2′*S*)-(*P*)-stable *trans*-**3** in a ratio of 90 : 6 : 0 : 4. Normally, photoisomerization of a stable motor molecule would lead to a clean *cis–trans* isomerization and a change in the orientation of the methyl substituent from (pseudo-)axial to (pseudo-)equatorial. This unexpected photochemical isomerization ((2′*S*)-(*M*)-*trans*-**3** to (2′*S*)-(*M*)-*cis*-**3**) is an additional pathway in this system. However, all four stages can be reached by a combination of photochemical and thermal stimuli.

In conclusion, we have demonstrated that the rate of rotation of the *o*-xylyl rotor of the molecular gearbox **3** could effectively be manipulated using light and heat as external triggers to control the isomerization behavior of the central double bond. It was shown by EXSY NMR techniques that for all four different states of the motor, the cogwheel had a different rate of rotation (stable *cis*-**3** > unstable *cis*-**3** > stable *trans*-**3** > unstable *trans*-**3**). Although the addressability of the stages of the motor is delicate and more complicated as in the second generation motors, the molecular gearbox serves as a proof of principle and shows that external control over coupled molecular rotary movement can be obtained.

Experimental

General remarks

The high-resolution one- and two-dimensional ^{1}H NMR spectra were obtained using a Varian VXR-300 and a Varian Unity Plus Varian-500 operating at 299.97 and 499.86 MHz, respectively, for the ^{1}H nucleus. ^{13}C NMR spectra were recorded on a Varian VXR-300 operating at 75.43 MHz. Chemical shifts are reported in δ units (ppm) relative to the residual deuterated solvent signals of $CHCl_3$ (^{1}H NMR: δ 7.26 ppm; ^{13}C NMR: δ 77.0 ppm), benzene (^{1}H NMR: δ 7.15 ppm; ^{13}C NMR: δ 128.0 ppm) and toluene (^{1}H NMR: δ 2.08 ppm). The splitting patterns are designated as follows: s (singlet), d (doublet), t (triplet), q (quartet), m (multiplet) and br (broad). One-dimensional ^{1}H NMR spectra were recorded using the acquisition parameters: $\pi/2$ pulse width, 6.5 μs; spectral width, 6.000 Hz; data size, 16 K; recycling delay, 1 s; number of transients, 32; temperature 298 K. All 2D spectra were collected as 2D hyper-complex data. After weighting with shifted sine-bell functions, the data were Fourier transformed in the absolute value mode using standard Varian VnmrS/VnmrX software packages. Two-dimensional phase-sensitive ^{1}H–^{1}H nuclear Overhauser enhancement spectra (NOESYPH) for NMR exchange experiments were obtained at 500 MHz with the acquisition parameters: $\pi/2$ pulse width, 6.5 μs; spectral width, 6.000 Hz; recycling delay, 1.0 s. The data were 512 w in the *F*1 dimension and 1 K in the *F*2 dimension and were zero-filled in *F*1 prior to two-dimensional Fourier transformation to yield a 1 K × 1 K data matrix. The spectra were processed using shifted sine-bell window functions in both dimensions. The measurements were conducted at 25, 35, 45 and 55 °C consisting of an arrayed cluster of mixing times (t_m = 0.05, 0.1, 0.2, 0.3, 0.5, 0.7, 1.0 and 1.5 s) per temperature.[19,20] The initial rate approximation was used for calculation of rate constants for the case of slow exchange between two equally populated sites and in the absence of scalar (*J*-modulated) spin–spin coupling. Peak integrals were determined by means of integration of the cross-(a_{AB} and a_{BA}) and auto-signals (a_{AA} and a_{BB}). UV–Vis measurements were performed on a Hewlett-Packard HP 8453 FT spectrophotometer and CD spectra were recorded on a JASCO J-715 spectropolarimeter using Uvasol grade solvents (Merck). MS (EI) and HRMS (EI) spectra were obtained with a Jeol JMS-600 spectrometer. Column chromatography was performed on silica gel (Aldrich 60, 230–400 mesh). HPLC analyses were performed on a Shimadzu HPLC system equipped with two LC-10AD*vp* solvent delivery systems, a DGU-14A degasser, a SIL-10AD*vp* autosampler, a SPD-M10A UV–Vis photodiode array detector, a CTO-10A*vp* column oven and a SCL-10A*vp* controller unit using silica and Chiralcel OD (Daicel) columns. Preparative HPLC was performed on a Gilson HPLC system consisting of a 231XL sampling injector, a 306 (10SC) pump, an 811C dynamic mixer, an 805 manometric module, with a 119 UV–Vis detector and a 202 fraction collector, using silica and Chiralcel OD (Daicel) columns. Elution speed was 1 ml min^{-1}. Irradiation experiments were performed with a 180 W Oriel Hg-lamp using a pyrex filter or filters of the appropriate wavelengths. Photostationary states were ensured by monitoring composition changes in time by taking UV–Vis spectra at distinct intervals until no changes were observed. Thermal helix inversions were monitored by CD spectroscopy using the apparatus described above and a JASCO PFD-350S/350L Peltier type FDCD attachment with a temperature control.

***trans*- and *cis*-2-(2″,6″-Dimethylphenyl)-9-(2′,3′-dihydro-2′-methyl-1*H*′-naphtho[2,1-*b*]thiopyran-1′-ylidene)-9*H*-thioxanthene (3).** The alkene **3** was synthesized by refluxing episulfide **6** (80 mg, 0.15 mmol) in the presence of triphenylphosphine (48 mg, 0.18 mmol) in *p*-xylene overnight. Purification was performed by column chromatography (SiO_2, hexane: CH_2Cl_2 = 4 : 1, R_f = 0.60) to give the desired product as a colorless oil (67 mg,

0.13 mmol, 89%) as a mixture of *cis* and *trans*-isomers in a ratio of 3.5 to 1; *m/z* (EI,%) = 512 (M^+, 100), 314 (38); HRMS (EI): calcd. for $C_{35}H_{28}S_2$: 512.1613, found 512.1632. Separation of the *cis*-**3** and *trans*-**3** isomers was performed using preparative HPLC using a silica column as the stationary phase and heptane as the eluent. The first eluted fraction (t = 9.7 min) contained *cis*-**3** and the second eluted fraction (t = 11.6 min) contained *trans*-**3** as was determined by ^{1}H NMR.

(2′*S)-(*P**)-*trans*-2-(2″,6″-Dimethylphenyl)-9-(2′,3′-dihydro-2′-methyl-1*H*′-naphtho[2,1-*b*]thiopyran-1′-ylidene)-9*H*-thioxanthene (3).** ^{1}H (300 MHz, $CDCl_3$) δ = 0.80–0.82 (d, J = 6.6 Hz, 3H), 1.97 (s, 3H), 2.22 (s, 3H), 2.94–2.99 (dd, J = 11.4, 3.5 Hz, 1H), 3.53–3.59 (dd, J = 11.4, 7.7 Hz, 1H), 4.15–4.21 (ddq, J = 7.7, 3.5, 6.6 Hz, 1H), 6.40–6.45 (m, 2H), 6.73–6.79 (dt, J = 7.3, 1.8 Hz, 1H), 6.98–7.04 (m, 1H), 7.07–7.24 (m, 5H), 7.31–7.40 (m, 3H), 7.54–7.61 (m, 2H), 7.58–7.60 (d, J = 8.4 Hz, 1H), 7.66–7.69 (d, J = 8.1 Hz, 1H); ^{1}H (300 MHz, benzene-d_6) δ = 0.56–0.58 (d, J = 6.6 Hz, 3H), 1.80 (s, 3H), 2.19 (s, 3H), 2.44–2.48 (dd, J = 11.2, 2.9 Hz, 1H), 3.02–3.08 (dd, J = 11.2, 7.5 Hz, 1H), 4.09–4.15 (m, 1H), 6.14–6.19 (m, 1H), 6.38–6.43 (m, 1H), 6.64–6.66 (d, J = 8.1 Hz, 1H), 6.77–6.80 (d, J = 8.1 Hz, 1H), 6.88–7.50 (m, 11H), 7.96–7.99 (d, J = 8.4 Hz, 1H); ^{13}C (75 MHz, $CDCl_3$) δ = 19.2 (q), 20.9 (q), 21.0 (q), 32.7 (d), 37.2 (t), 124.35 (d), 124.42 (d), 125.3 (d), 125.6 (d), 125.8 (d), 126.1 (d), 126.4 (d), 127.31 (d), 127.37 (d), 127.49 (d), 127.52 (d), 127.6 (d), 128.1 (d), 129.0 (d), 130.8 (s), 131.4 (s), 131.5 (s), 132.5 (s), 134.3 (s), 135.3 (s), 135.9 (s), 136.1 (s), 136.3 (s), 136.7 (s), 138.3 (s), 139.1 (s), 141.0 (s), one singlet and two doublets were not observed in the aromatic region due to overlap; UV–Vis: (*n*-hexane) λ (ε) 222 (50 300), 262 (29 800), 324 (7500). The enantiomers of (2′*S**)-(*P**)-*trans*-**3** were separated by chiral preparative HPLC using a Daicel Chiralcel OD column as the stationary phase and a mixture of heptane : i-propanol in a ratio of 99.5 : 0.5 as the eluent. The first eluted fraction (t = 7.2 min) contained (2′*S*)-(*P*)-*trans*-**3** and the second eluted fraction (t = 8.4 min) contained (2′*R*)-(*M*)-*trans*-**3**; CD: (2′*S*)-(*P*)-*trans*-**3** (*n*-hexane) λ $\Delta\varepsilon$) 224.2 (+69.1), 243.8 (−10.3), 250.2 (+14.3), 270.8 (−128.4), 316.0 (+16.6).

(2′*S)-(*P**)-*cis*-2-(2″,6″-Dimethylphenyl)-9-(2′,3′-dihydro-2′-methyl-1*H*′-naphtho[2,1-*b*]thiopyran-1′-ylidene)-9*H*-thioxanthene (3).** ^{1}H (300 MHz, $CDCl_3$) δ = 0.66–0.68 (d, J = 7.0 Hz, 3H), 0.77 (s, 3H), 1.69 (s, 3H), 3.05–3.10 (dd, J = 11.4, 2.6 Hz, 1H), 3.65–3.71 (dd, J = 11.4, 7.3 Hz, 1H), 4.06–4.12 (ddq, J = 7.3, 2.6, 7.0 Hz, 1H), 6.39–6.40 (d, J = 1.8 Hz, 1H), 6.53–6.56 (dd, J = 8.1, 1.8 Hz, 1H), 6.80–6.83 (d, J = 7.3 Hz, 1H), 6.87–6.89 (d, J = 7.0 Hz, 1H), 6.96–7.01 (t, J = 7.5 Hz, 1H), 7.11–7.19 (m, 2H), 7.28–7.40 (m, 4H), 7.54–7.62 (m, 3H), 7.66–7.69 (dd, J = 7.5, 1.3 Hz, 1H), 7.76–7.79 (d, J = 8.8 Hz, 1H); ^{1}H (300 MHz, benzene-d_6) δ = 0.42–0.44 (d, J = 6.6 Hz, 3H), 1.04 (s, 3H), 1.56 (s, 3H), 2.53–2.59 (dd, J = 11.4, 2.6 Hz, 1H), 3.19–3.25 (dd, J = 11.4, 7.7 Hz, 1H), 3.89–3.94 (m, 1H), 6.36–6.39 (d, J = 8.1 Hz, 1H), 6.73–7.41 (m, 13H), 7.48–7.50 (d, J = 7.7 Hz, 1H), 8.14–8.16 (d, J = 8.1 Hz, 1H); ^{13}C (75 MHz, $CDCl_3$) δ = 19.0 (q), 19.9 (q), 20.7 (q), 32.1 (d), 37.0 (t), 124.5 (d), 125.9 (d), 126.1 (d), 126.65 (d), 126.7 (d), 126.9 (d), 127.2 (d), 127.6 (d), 127.8 (d), 127.9 (d), 128.9 (d), 130.5 (s), 131.1 (s), 132.0 (s), 132.8 (s), 134.8 (s), 135.9 (s), 136.2 (s), 136.3 (s), 136.5 (s), 139.0 (s), 139.1 (s), 140.6 (s), due to overlap in the aromatic region, five (d) and two (s) signals were not observed; UV–Vis: (*n*-hexane) λ (ε) 221 (50 900), 248 (30 400), 321 (7200). The enantiomers of (2′*S**)-(*P**)-*cis*-**3** were separated by preparative chiral HPLC using a Daicel Chiralcel OD column as the stationary phase and a mixture of heptane : i-propanol in a ratio of 99.5 : 0.5 as the eluent. The first eluted fraction (t = 7.2 min) contained (2′*S*)-(*P*)-*cis*-**3** and the second eluted fraction (t = 8.4 min) contained (2′*R*)-(*M*)-*cis*-**3**; CD: (2′*S*)-(*P*)-*cis*-**3** (*n*-hexane): λ ($\Delta\varepsilon$) 225.2 (+115.2), 243.0 (−6.3), 253.0 (+25.8), 276.0 (−119.7), 314.6 (+10.5), 344.0 (+11.9).

(2′*S)-(*M**)-*trans*-2-(2″,6″-Dimethylphenyl)-9-(2′,3′-dihydro-2′-methyl-1*H*′-naphtho[2,1-*b*]thiopyran-1′-ylidene)-9*H*-thioxanthene (3).** ^{1}H (300 MHz, benzene-d_6) δ = 0.98–1.01 (d, J = 7.3 Hz, 3H), 1.65 (s, 3H), 2.19 (s, 3H); ^{1}H (500 MHz, $CDCl_3$) δ = 1.26–1.28 (d, J = 6.6 Hz, 3H), 1.92 (s, 3H), 2.26 (s, 3H); the remaining signals could not be assigned with certainty due to the presence of other isomers of **3**.

(2′*S)-(*M**)-*cis*-2-(2″,6″-Dimethylphenyl)-9-(2′,3′-dihydro-2′-methyl-1*H*′-naphtho[2,1-*b*]thiopyran-1′-ylidene)-9*H*-thioxanthene (3).** ^{1}H (300 MHz, benzene-d_6) δ = 0.78–0.81 (d, J = 7.3 Hz, 3H), 1.02 (s, 3H), 1.52 (s, 3H), 2.11–2.20 (m, 1H), 2.80–2.92 (m, 2H), 6.34–6.37 (d, J = 8.1 Hz, 1H), 6.72–7.47 (m, 14H), 7.99–8.02 (d, J = 8.4 Hz, 1H); ^{1}H (500 MHz, $CDCl_3$) δ = 0.55 (s, 3H), 1.09–1.12 (d, J = 6.6 Hz, 3H), 1.70 (s, 3H); the remaining signals could not be assigned with certainty due to the presence of other isomers of **3**; UV–Vis characteristics of the PSS (*n*-hexane): λ (ε) 218 (53 000), 264 (30 300); CD: characteristics for the PSS generated from (2′*S*)-(*P*)-**3** (*n*-hexane): λ ($\Delta\varepsilon$) 226.4 (−64.8), 243.8 (+23.3), 254.6 (−26.2), 277 (+80.9), 350.2 (−14.4).

Dispiro[2,3-dihydro-2′-methyl-1*H*-naphtho[2,1-*b*]-thiopyran-1,2′-thiirane-3′,9″-[2″-(2,6-dimethylphenyl)-9″*H*-thioxanthene]] (6). To a solution of hydrazone **4** (61.2 mg, 0.25 mmol) in CH_2Cl_2 (10 ml) under nitrogen were subsequently added $MgSO_4$ (300 mg), Ag_2O (150 mg) and a saturated solution of KOH in methanol (5 drops) at 0 °C. Stirring this mixture for 30 min at 0 °C gave a dark red solution. If only a slightly red color was observed, more Ag_2O and KOH in methanol were added. The solution was then filtered into another ice-cooled flask after which a solution of appropriate thioketone **5** (54.7 mg, 0.160 mmol) in CH_2Cl_2 was added. Most of the time, the evolution of nitrogen gas could be observed. Stirring was continued for 2 h at 0 °C and then for 4 h at room temperature. Evaporation of the CH_2Cl_2 then gave a residue which was used for further purification. The episulfide **6** was obtained as a colorless solid (80.0 mg, 0.147 mmol, 92%) after column chromatography (SiO_2, hexanes : CH_2Cl_2 = 1 : 1, R_f = 0.81) as a mixture of a *cis*- and *trans*-isomers in a ratio of 3.5 : 1; ^{1}H (300 MHz, $CDCl_3$) δ = 0.98 (s, 3H, *cis*), 1.03–1.05 (d, J = 6.6 Hz, 3H, *cis*), 1.16–1.19 (d, J = 7.2 Hz, 3H, *trans*), 1.71 (s, 3H, *cis*), 2.02 (s, 3H, *trans*), 2.10 (s, 3H, *trans*), 2.17–2.73 (m, 3H *cis*, 3H, *trans*), 6.23–6.29 (dt, J = 7.1, 1.1 Hz, 1H, *trans*), 6.58–6.62 (dd, J = 7.9, 1.7 Hz, 1H, *cis*), 6.73–6.78 (dt, J = 7.3, 1.1 Hz, 1H, *trans*), 6.81–7.60 (m, 13H, *cis*, 12H, *trans*), 7.82–7.83 (d, J = 1.8 Hz, 1H, *trans*), 8.04–8.08 (dd, J = 5.9, 3.7 Hz, 1H, *cis*), 8.84–8.87 (d, J = 8.8 Hz, 1H, *trans*), 8.92–8.95 (d, J = 8.8 Hz, 1H, *cis*); *m/z* (EI,%) = 544 (M^+, 66), 512 (100), 501 (40), 496 (18), 370 (21), 314 (39), 301 (45); HRMS (EI): calcd. for $C_{35}H_{28}S_3$: 544.1353, found 544.1340.

References

1 (*a*) V. Balzani, M. Venturi, A. Credi, *Molecular Devices and Machines: A Journey into the Nanoworld*, Wiley-VCH, Weinheim, 2004; (*b*) Special Issue of Scientific American: Nanotech, The Science of the Small Gets Down to Business, September 2001; (*c*) *Acc. Chem. Res.*, Special issue (Molecular Machines), 2001, **34**(6).

2 (*a*) P. D. Boyer, *Angew. Chem., Int. Ed.*, 1998, **37**, 2296–2307; P. D. Boyer, *Angew. Chem.*, 1998, **110**, 2424–2436; (*b*) J. E. Walker, *Angew. Chem., Int. Ed.*, 1998, **37**, 2308–2319; J. E. Walker, *Angew. Chem.*, 1998, **110**, 2438–2450.

3 (*a*) N. Koumura, R. W. J. Zijstra, R. A. van Delden, N. Harada and B. L. Feringa, *Nature*, 1999, **401**, 152–155; (*b*) T. R. Kelly, H. De Silva and R. A. Silva, *Nature*, 1999, **401**, 150–152; (*c*) D. A. Leigh, J. K. Y. Wong, F. Dehez and F. Zerbetto, *Nature*, 2003, **424**, 174–179.

4 (*a*) H. Iwamura and K. Mislow, *Acc. Chem. Res.*, 1988, **21**, 175–182; (*b*) O. S. Akkerman, *Recl. Trav. Chim. Pays-Bas*, 1970, **89**, 673–679.

5 (*a*) T. C. Bedard and J. S. Moore, *J. Am. Chem. Soc.*, 1995, **117**, 10662–10671; (*b*) T. R. Kelly, M. C. Bowyer, K. V. Bhaskar, D. Bebbington, A. Garcia, F. Lang, M. H. Kim and M. P. Jette, *J. Am. Chem. Soc.*, 1994, **116**, 3657–3658; (*c*) A. M. Schoevaars, W. Kruizinga,

R. W. J. Zijlstra, N. Veldman, A. L. Spek and B. L. Feringa, *J. Org. Chem.*, 1997, **62**, 4943–4948; (*d*) Z. Dominguez, H. Dang, M. J. Strouse and M. A. Garcia-Garibay, *J. Am. Chem. Soc.*, 2002, **124**, 2398–2399; (*e*) C. Joachim and J. K. Gimzewski, *Struct. Bonding*, 2001, **99**, 1–18; (*f*) H. Jian and J. M. Tour, *J. Org. Chem.*, 2003, **68**, 5091–5103; (*g*) T. K. Tashiro, K. Konishi and T. Aida, *J. Am. Chem. Soc.*, 2000, **122**, 7921–7926; (*h*) X. Zheng, M. E. Mulcahy, D. Horinek, F. Galeotti, T. F. Magnera and J. Michl, *J. Am. Chem. Soc.*, 2004, **126**, 4540–4542; (*i*) M. Takeuchi, M. Ikeda, A. Sugasaki and S. Shinkai, *Acc. Chem. Res.*, 2001, **34**, 865–873; (*j*) *Molecular Catenanes, Rotaxanes and Knots*, ed. J.-P. Sauvage, C. Dietrich-Buchecker, Wiley-VCH, Weinheim, 1999; (*k*) G. S. Kottas, L. I. Clark, D. Horinek and J. Michl, *Chem. Rev.*, 2005, **125**, 1281–1376.

6 (*a*) N. Koumura, E. M. Geertsema, A. Meetsma and B. L. Feringa, *J. Am. Chem. Soc.*, 2000, **122**, 12005–12006; (*b*) N. Koumura, E. M. Geertsema, M. B. van Gelder, A. Meetsma and B. L. Feringa, *J. Am. Chem. Soc.*, 2002, **124**, 5037–5051.

7 M. K. J. ter Wiel, J. Vicario, S. G. Davey, A. Meetsma and B. L. Feringa, *Org. Biomol. Chem.*, 2005, **3**, 28–30.

8 We have no clear explanation for the preferred formation of *cis*-**3**. It is anticipated that the intermediate thiocarbonyl ylide undergoes rotation to provide the most stableepisulfide leading, after sulfur extrusion, to *cis*-**3** as the major isomer.

9 The asterisk (*) denotes the use of racemic compounds and is used to clarify the relation between the helicity of the molecule and the absolute configuration of the carbon atom of the stereogenic center. For example, for an alkene with a methyl substituent, (2′*S**)-(*P**)-*trans* means that the alkene is a racemic mixture of two enantiomers, (2′*S*)-(*P*)-*trans* and (2′*R*)-(*M*)-*trans*, of a stable *trans*-isomer, whereas for the same alkene, (2′*R**)-(*P**)-*trans* would indicate that the molecule is a racemic mixture of an unstable *trans*-isomer consisting of the (2′*R*)-(*P*)-*trans* and (2′*S*)-(*M*)-*trans* enantiomers. From this example it is important to note that a combination of the absolute configuration at the stereogenic carbon atom (*R* or *S*) and the overall helicity of the molecule (*P* or *M*) is only valid for certain combinations, since different isomers, stable or unstable, can be meant.

10 Crystal data for **3**: $C_{35}H_{28}S_2$; $M = 512.74$; colorless, platelet; monoclinic; space group $P2_1/c$; $a = 15.654(1)$, $b = 11.310(1)$, $c = 15.827(1)$ Å; $\beta = 113.376(1)°$; $V = 2572.1(3)$ Å^3; $Z = 4$; $\rho_{calc} = 1.324$ g cm^{-3}; $T = 100(1)$ K; $\mu = 2.31$ cm^{-1}; number of reflections: 4390; number of refined parameters: 446; final agreement factors: $wR(F^2) = 0.1595$, $R(F) = 0.0630$, GoF = 1.075. CCDC 271760 contains the supplementary crystallographic data for this paper.vadjust

11 (*a*) G. Bodenhausen, H. Kogler and R. R. Ernst, *J. Magn. Reson.*, 1984, **58**, 370–388; (*b*) J. Jeener, B. M. Meier, P. Bachmann and R. R. Ernst, *J. Chem. Phys.*, 1979, **71**, 4546–4553; (*c*) S. Macura and R. R. Ernst, *Mol. Phys.*, 1980, **41**, 95–117; (*d*) G. Bodenhausen and R. R. Ernst, *J. Am. Chem. Soc.*, 1982, **104**, 1304–1309.

12 According to the initial rate approximation method proposed by Ernst and co-workers,[11] the rate of exchange (rate of rotation k) can be calculated directly from the ratio of cross-(a_{AB} and a_{BA}) and autopeak integrations (a_{AA} and a_{BB}) and the mixing time using the formula $(a_{AA}/a_{AB}) = (1\text{-}kt_m)/kt_m$, provided a slow exchange situation and absence of scalar spin–spin coupling. This equation can be transformed into $k = 1/t_m \cdot (a_{AB}/(a_{AA} + a_{AB}))$. A plot of t_m *versus* $(a_{AB}/(a_{AA} + a_{AB}))$ will therefore directly give the rate constant k at a given temperature. These k-values can be used subsequently to determine the thermodynamic parameters, $\Delta^{\ddagger}G^0$, $\Delta^{\ddagger}H^0$ and $\Delta^{\ddagger}S^0$, *via* an Eyring plot ($\ln(kh/k_bT)$ *versus* $1/T$).

13 Where possible, the average value of the two cross-peaks a_{AB} and a_{BA} was used in order to minimize the error margin. At 45 and 55 °C, however, an overlap of the *o*-xylyl moiety methyl absorption at highest field in *cis*-**3** with the absorption of the methyl substituent in the upper half occurred. Since this disturbance makes an accurate determination of the rate constant impossible, these signals were no longer taken into account.

14 Irradiation in $CDCl_3$ is not ideal, but for short irradiation times the amount of side products generated is limited.

15 For both the unstable *trans*-**3** and unstable *cis*-**3** only one cross-peak could be used to determine the rate constant. The other cross-peaks were not used due to overlap with other resonances.

16 For a molecular rotor, the rate of rotation for the *cis*-isomer was also found to be higher than the rate of rotation for the *trans*-isomer[5c].

17 *Cis*- and *trans*-**3** were separated by preparative HPLC over a silica column using heptane as the eluent. The enantiomers of *cis*-**3** and *trans*-**3** were then separated by a second preparative HPLC column using a Chiralcel OD-column as the stationary phase and a mixture of heptane and i-propanol in a ratio of 99 : 1 as the eluent. The absolute configuration of the first eluted fractions was in both cases assigned to be (2′*S*)-(*P*) by comparison with related compounds.

18 Accurate kinetic measurements could not be performed in *n*-hexane due to the high volatility.

19 (*a*) R. Willem, *Prog. Nucl. Magn. Reson. Spectrosc.*, 1987, **20**, 1–94; (*b*) K. G. Orrell, V. Sik and D. Stephenson, *Prog. Nucl. Magn. Reson. Spectrosc.*, 1990, **22**, 141–208.

20 (*a*) P. W. Kuchel, B. T. Bulliman, B. E. Chapman and G. L. Mendz, *J. Magn. Reson.*, 1988, **70**, 34–53; (*b*) C. L. Perrin, *J. Magn. Reson.*, 1989, **82**, 619–621.